



# Temperate dryland vegetation changes under a warming climate and strong human intervention – With a particular reference to the district Xilin Gol, Inner Mongolia, China



Hongwei Li<sup>\*</sup>, Xiaoping Yang<sup>\*</sup>

Key Laboratory of Cenozoic Geology and Environment, Institute of Geology and Geophysics, Chinese Academy of Sciences, P.O. Box 9825, Beijing 100029, China

## ARTICLE INFO

### Article history:

Received 13 August 2013

Received in revised form 21 December 2013

Accepted 7 March 2014

Available online xxxx

### Keywords:

Desertification

NDVI

Global warming

Semi-arid environment

Inner Mongolia

## ABSTRACT

Assessment of the dryland vegetation change and identifying its causes are of great importance for combating desertification and projecting future ecosystem dynamics in arid and semiarid regions. Since plant growth in temperate drylands is constrained by both water and temperature, understanding how ongoing warming climate will impact temperate vegetation of the steppe and fixed dune fields is a crucial question requiring great attention from both scientific communities and decision makers. In this study, we aimed to provide a reliable evaluation of the recent status and trends of desertification in the 142,400 km<sup>2</sup> Xilin Gol district of eastern Inner Mongolia located in the east portion of Asian mid-latitude desert belt. Data sources included the Normalized Difference Vegetation Index (NDVI) time series from the period 1982 to 2006 and climate records from 17 local weather stations, supported by more recent ground checking. Our results show that there is little significant decrease of vegetation greenness on annual time scales under recent warming climate; however a human-induced browning trend occurs in May and June, associated with limited water availability. Results indicate that year round warming exacerbates water deficits in spring and early summer damaging vegetation. This impact is especially pronounced in desert steppe areas. Although both temperature and precipitation are projected to increase over the study area in coming decades, our work demonstrates that it is unlikely that vegetation losses from degradation will be reduced under the current climate change trends.

© 2014 Elsevier B.V. All rights reserved.

## 1. Introduction

Drylands, which encompass regions classified as dry subhumid, semiarid, arid, or hyperarid, are characterized by high climate variability and sensitive responses to climate fluctuations and human management. Their vulnerability, as evidenced by the droughts that occurred in the Sahel during the last decades (Hulme, 2001; Nicholson, 2001), can produce drastic consequence for the humans and their livestock. Dryland vegetation condition is an effective indicator of the land degradation, and maintaining its health is a key preventive measure against desertification (Millennium Ecosystem Assessment, 2005).

In the last century, the Northern Hemisphere, particularly the mid-to-high latitudes, experienced a warming trend partly attributed to global warming (IPCC, 2007) with increasing drought and aridity in some regions, including North China (Dai, 2011; Lei and Duan, 2011; Ma and Fu, 2006; Zou et al., 2005). Unlike vegetation in tropical drylands, which is primarily determined by rainfall, plant growth in the temperate dryland is constrained by both water and temperature (Nemani et al., 2003). Since rising temperatures may extend growing season (Piao et al., 2006a;

Tucker et al., 2001; Yu et al., 2003) and exacerbate moisture deficits through evaporation and reduction of snow cover (Brown, 2000; Peng et al., 2010), precise knowledge of vegetation variability is of great significance for understanding the response of dryland ecosystems to global warming.

Despite several national programs to combat desertification (CCICCD, 2006), the trend of desertification in China is debated. According to a national report (CCICCD, 2000), desertification spread with an accelerating rate from the 1950s to 1990s, with human activity deemed to be the primary cause. Similar conclusions have been shown in other comprehensive studies (Wang et al., 2004a; Zhu and Wang, 1990). However, Zhong (1999) has argued that shifting sands in China have tended to stabilize since 1950s possibly indicating a slowing or even reversal of desertification processes. Vegetation indices derived from remote sensing data also suggest a reversal in desertification in the 1980s to 1990s in arid and semiarid China, which was attributed to the wetting trend (Piao et al., 2005). The status and severity of desertification at regional scales have also been the subject of debate with a range of inconsistent results. For instance, Liu et al. (2008) utilizing remote sensing data from the years 1987, 2000 and 2006, came to the conclusion that the area of active dunes in Hunshandake Sandy Land increased by 2622 km<sup>2</sup> from 1987 to 2000. Yang et al. (2007), however, have suggested that extensions of wetlands and desertified lands have

<sup>\*</sup> Corresponding authors. Tel.: +86 10 82998387.

E-mail addresses: [lihwo8@mail.iggcas.ac.cn](mailto:lihwo8@mail.iggcas.ac.cn) (H. Li), [xpyang@mail.iggcas.ac.cn](mailto:xpyang@mail.iggcas.ac.cn) (X. Yang).

fluctuated in response to the regional variations in temperature and precipitation.

The controversial debate on desertification trends can be largely ascribed to a lack of indicators that quantitatively, directly, and comprehensively can show dryland degradation/desertification. Although vegetation is not the only indicator of desertification, it is the one most frequently used since vegetation variation can be monitored from the continuous remote sensing records that are available for the past three decades. In this paper, the remotely sensed Normalized Difference Vegetation Index (NDVI) for the period 1982–2006 is used as a proxy of greenness to monitor monthly vegetation variations in Xilin Gol, eastern Inner Mongolia, a region widely considered as having severe desertification (Fig. 1). We also considered different vegetation types and aimed to identify the divergent response of each to climate change and human management. Our results should provide a solid base for assessing the state and trends of desertification in northern China.

## 2. Regional setting

The Xilin Gol district of Inner Mongolia, 142,400 km<sup>2</sup> in area, is located between the latitudes 42° N and 45.5° N and the longitudes 111° E and 118° E in the eastern part of the Asian mid-latitude desert belt (Yang et al., 2012; Fig. 1). Elevation increases gently from 900 to 1000 m in the northwest to 1500 to 2000 m in the southeast. The Hunshandake (Otindag) Sandy Land, a dune field covering an area of 21,400 km<sup>2</sup>, lies in the southern part of the Xilin Gol (Fig. 1). Parabolic, linear, network and barchan dunes with heights of up to 30 m occur in the sandy land. Currently, most of the dunes are semi-stabilized to well-stabilized by vegetation (Liu and Yang, 2013; Yang et al., 2012; Zhu et al., 1980).

The climate of the study area is arid in the west and semiarid elsewhere. Mean annual precipitation decreases gradually from 400 mm in the southeast to 100 mm in the west. Characterized by remarkable seasonality, summer (June to August) rains provide as much as 60–70% of the annual precipitation (Fig. 1). The region is also marked by high inter-annual variability with the coefficient of variation of annual precipitation reaching 20–35% in the study area. Compared to other parts of the Asian mid-latitude desert belt, the mean annual temperature of the study area, ranging from 0 to 5.5 °C, is much lower. Subzero mean monthly temperatures last from November to March, with January averages dropping to as low as –20 °C and rising to over 20 °C in July (Fig. 1).

Because of the asynchronous timing of the energy and water supply, May is the relatively dry month for the study area with the dry season longer in the west part than in the east (climatic diagram of Walter and Lieth, 1960) (Fig. 1). In the study area, most rivers and ephemeral streams flowing from the surrounding mountains dry up in the desert. Prevailing winds are primarily from northwest and west, the annual average wind speed decreases from 5 m/s in the west to the 3 m/s in the east, forming desert pavements in the west and sand accumulations in the mountains in the east even far beyond the Sandy Land.

Vegetation distribution is controlled by the water availability in the study area with desert steppe and arid steppe comprising the major vegetation types and accounting for 27% and 43% of the study area, respectively (Fig. 1). Desert steppe, dominated by *Stipa gobica* and *Stipa klemenzii*, prevails in the west where mean annual precipitation is below 200 mm. Arid steppe occurs in the mid-east with mean annual precipitation ranging from 200 mm to 350 mm with *Leymus chinensis*, *Stipa grandis*, *Stipa krylovii*, *Agriophyllum squarrosum*, *Bassia dasyphylla* and *Corispermum* the predominant plant species. Trees and shrubs, mainly *Quercus mongolica*, *Betula platyphylla*, *Populus davidiana*, *Ulmus macrocarpa*, *Caragana* spp. and *Ostryopsis davidiana*, are found in the eastern mountains and lee slopes of the stable dunes. Meadow steppe and meadow primarily occur in the transition zone between forest and steppe and along the rivers, respectively. Additionally, bare desert patches surrounded by desert steppe are found in the west and cropland occurs in the southern and eastern margin of the study area.

## 3. Materials and methods

### 3.1. Datasets

#### 3.1.1. Normalized Difference Vegetation Index (NDVI)

Normalized Difference Vegetation Index (Tucker, 1979) is defined as follows:

$$NDVI = \frac{(\rho_{NIR} - \rho_R)}{(\rho_{NIR} + \rho_R)}$$

where  $\rho_{NIR}$  and  $\rho_R$  are the spectral reflectance in the near infrared and red band, respectively. NDVI contrasts the green leaf's absorption on the two bands and becomes a measure of chlorophyll abundance and energy absorption (Myneni et al., 1995). Research has shown that

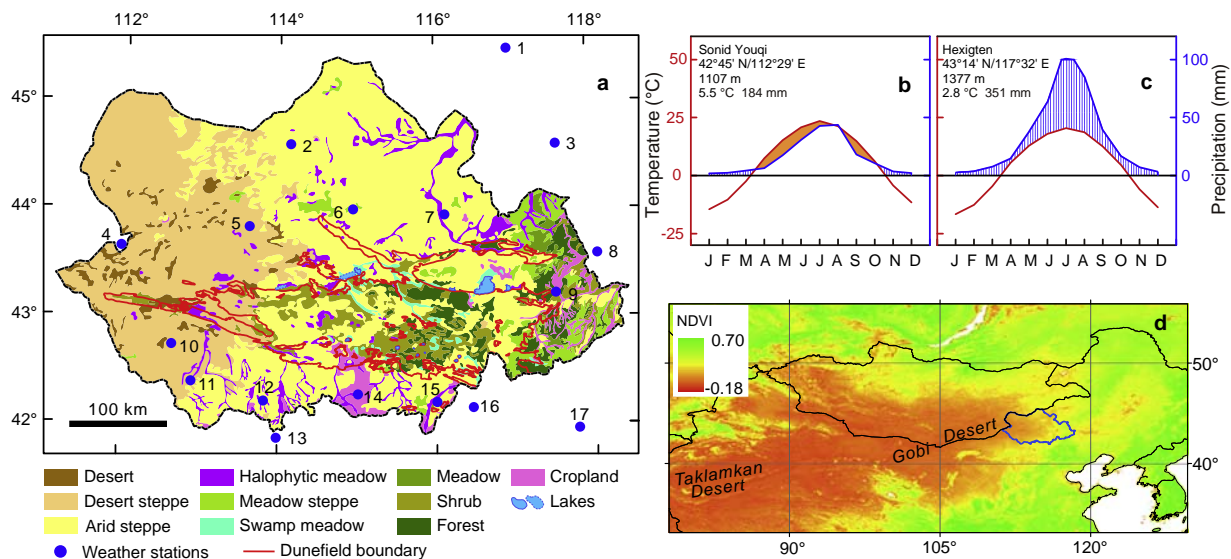


**Fig. 1.** Overview of the study area. (a) Vegetation types. (b–c) Walter–Lieth climate diagrams (following Walter and Lieth, 1960) of No. 10 and No. 9 weather stations (shown in panel a); the name, latitude, longitude, altitude, mean annual temperature and precipitation of each weather station are shown in the diagram. (d) Location of the study area with the distribution of mean annual NDVI.

NDVI correlates with biomass and productivity (Box et al., 1989; Paruelo et al., 1997; Wang et al., 2004b). In this study, we used the Global Inventory Modeling and Mapping Studies (GIMMS) Normalized Difference Vegetation Index (NDVI) time series derived from Advanced Very High Resolution Radiometer (AVHRR) instrument on-board the NOAA satellites to access vegetation variability and condition. The GIMMS NDVI product has been corrected for calibration effects, view geometry, volcanic aerosols, and other effects not related to vegetation change, and then formed into bimonthly maximum value composite (MVC) images (Pinzon et al., 2005; Tucker et al., 2005). Although the spatial resolution of GIMMS NDVI is only 8 km, it is the longest (1981–2006) vegetation record available. Its high temporal resolution makes it the main resource for investigation of terrestrial vegetation dynamics. Also, GIMMS NDVI performs better in the temporal change analysis than other available NDVI datasets (Beck et al., 2011; Slayback et al., 2003). The NDVI data applied used spans from 1982 to 2006 with a spatial resolution of 0.07272727° (GLCF, <ftp://ftp.glcfc.umd.edu/glcfc/GIMMS/Geographic>).

3.1.2. Climate data

We examined monthly precipitation and mean temperature from 17 weather stations in the study area downloaded from the China Meteorological Data Sharing Service System (<http://new-cdc.cma.gov.cn:8081/home.do>) and local meteorological administrations. Ordinary kriging (Stein, 1999) was applied to interpolate the climate data and was resampled at the same pixel size as the NDVI dataset.

3.1.3. Vegetation types

The vegetation data were acquired by digitizing the vegetation map of China at a scale of 1:1,000,000 (Editorial Board of Vegetation Map of China and Chinese Academy of Sciences, 2007). The data used to compile the map was collected from 1980s to 1990s, approximately coincided with the NDVI dataset.

3.1.4. Social-economic data

Grazing is the dominant land use practice in our study area and hence we use livestock data recorded by the local governments as an indicator of human intervention on the vegetation. According to statistical yearbooks and field investigations, livestock in the Xilin Gol include sheep, goat, cattle, horse and camels. In order to normalize grazing intensity among different species, we used an equivalent unit of grazing, i.e. “sheep unit”, proposed by the Ministry of Agriculture of People’s Republic of China (2002). According to this national standard, the transition factor for a sheep/goat, cattle, horse and camel is 0.7–1.2, 4.5–8,

5–6.5, and 7.5–8, respectively. In this paper, to simplify the calculation, we set the transition factor for cattle, horses and camels to be 6, whereas the factor was set to 1 for sheep and goats.

3.2. Methods

Growing season NDVI from April to October was used in the study with monthly and annual NDVI obtained by averaging the bimonthly NDVI data. Accordingly, annual climate data used in the study refer to the growing year (November to the next October) rather than the calendar year (January to December).

3.2.1. MK test and Sen’s slope

The Mann–Kendall (Kendall, 1975; Mann, 1945) (MK) test was applied in the trend analysis of the NDVI and climate data. MK is a non-parametric test that is more suitable for non-normally distributed data and censored data such as hydro-meteorological time series (Yue et al., 2002). The MK test compares the relative magnitude of the data and computes a Z statistic that follows the standard normalized distribution with the mean of zero and variance of one. Negative and positive values of Z represent increasing and decreasing trends, respectively. The magnitude of the trend was estimated by a nonparametric approach proposed by Sen (1968) and Theil (1992),

$$b = \text{Median} \left( \frac{X_j - X_i}{j - i} \right) \quad \forall j > i$$

where *b* is the estimated slope (Sen’s slope) of the trend and *X<sub>i</sub>* and *X<sub>j</sub>* are the *i*th and *j*th observations, respectively.

3.2.2. Correlation analysis

We applied different approaches to determine Pearson’s correlation coefficients (*r*) (Galton, 1886; Pearson, 1920) between vegetation growth and climate. Unlike the sensitive responses of vegetation to rainfall change in drylands, the relationship between NDVI and temperature tends to be obscured and even distorted by precipitation, which is due to the significant correlation both between rainfall and NDVI (see Section 4.4) and between rainfall and temperature. Usually, rainy weather is associated with lower temperatures and thus the correlation (*r*) between NDVI and temperature tends to be negative especially in summer months – reaching as low as –0.67 in the study area (*p* < 0.001, Supplementary Fig. S1). Thus the negative correlation between temperature and NDVI might not be indicative of vegetation favoring cooler climate.

**Table 1**  
Monthly temperature changes (°C) recorded by the weather stations in the study area for the period 1982–2006.

Weather station	Jan	Feb	Mar	Apr	May	Jun	Jul	Aug	Sep	Oct	Nov	Dec	Yearly
1 East Ujimqin	2.0	4.8*	3.6*	1.6	0.9	1.6	2.5***	1.8*	3.9***	1.1	0.8	–1.3	1.4***
2 Narenbaolage	1.6	3.7	3.4**	1.7	0.6	1.7*	2.5**	2.0*	3.1***	0.2	0.6	–0.7	2.5***
3 West Ujimqin	1.0	5.0**	3.1	2.1	0.6	0.9	2.1**	0.9	3.2***	1.1	0.8	–0.3	1.9***
4 Erenhot	2.2	4.3	3.5*	2.7*	0.6	2.8***	2.7***	2.7**	3.6***	1.3	2.2	0.5	2.3***
5 Sonid Zuoqi	–0.1	3.1	3.0*	2.0	0.8	2.6**	2.6**	2.7*	3.8***	0.3	1.0	–0.9	1.8***
6 Abag	2.6*	5.0**	3.9**	2.1	0.9	1.7	2.2**	1.6*	3.5***	0.7	1.3	0.9	1.4***
7 Xilinhot	0.8	5.1*	3.5*	1.5	0.6	1.1	1.8*	1.5	2.9***	0.8	0.0	–0.9	1.7***
8 Linxi	1.1	4.0**	2.6	2.0	0.5	0.9*	2.0**	0.5	2.5***	0.3	0.1	–1.3	1.3***
9 Hexigten	1.5	5.5**	3.1**	1.5	0.7	0.9	1.9**	0.6	2.2***	0.6	0.5	–0.4	1.9***
10 Sonid Youqi	2.0	4.4	2.9*	1.8	0.4	2.3**	1.9**	2.2*	2.9***	0.8	1.6	2.0	1.6***
11 Zhurihe	1.6	4.0	2.5	1.4	0.1	2.1**	1.4*	2.1*	2.8***	0.6	1.0	0.4	1.8***
12 Xianghuangqi	2.4	4.4*	1.8	1.6	0.3	1.9	1.9**	1.5*	2.7***	0.0	1.7	0.6	1.5***
13 Huade	1.6	3.7	2.3	1.3	0.0	1.5*	1.6*	3.6**	2.4***	0.0	1.3	0.6	1.4***
14 Zhengxiangbaiqi	2.8*	5.6**	2.7*	1.4	0.2	1.5	1.8**	1.3	2.8***	0.3	1.5	0.6	1.1***
15 Zhenglanqi	2.6*	4.9**	2.7	1.3	0.3	1.4*	1.7**	1.0	2.7***	0.3	1.3	0.8	1.5***
16 Duolun	2.2	5.0**	2.5*	1.3	0.5	1.3	1.6**	0.8	1.9***	0.3	1.2	0.7	2.0***
17 Weichang	1.5	3.9**	2.5	0.8	0.0	0.2	0.9	0.4	1.3**	0.0	0.5	–0.4	1.0***

For the locations of weather stations see Fig. 1. Single, double, and triple asterisks indicate temperature changes at a significance level (*p*) of 0.1, 0.05 and 0.01, respectively.

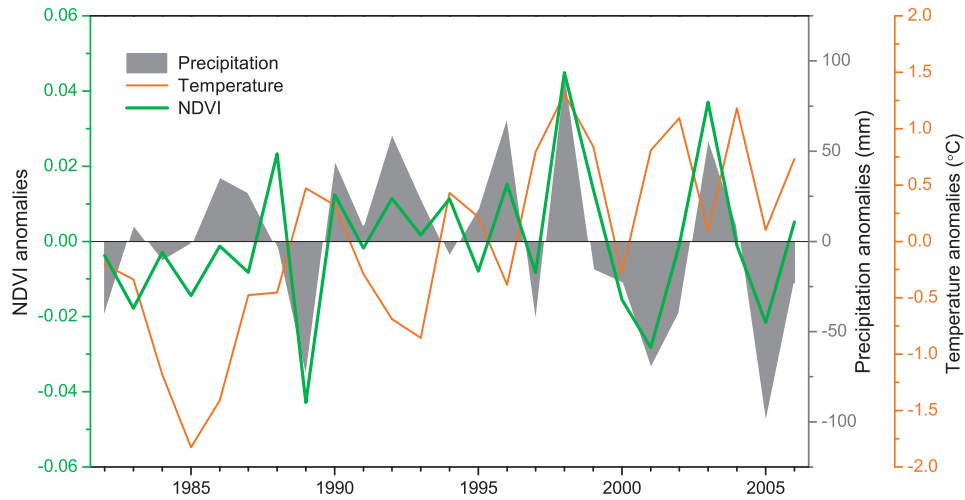


**Fig. 2.** Anomalies of mean annual precipitation, temperature and growing season (April–October) NDVI averaged over the study area for the period of 1982–2006. (For interpretation of the references to color in this figure, the reader is referred to the web version of this article.)

In order to eliminate precipitation effects, we used the residuals of NDVI and temperature produced by regression with precipitation, instead of the original NDVI and temperature dataset, to perform the correlation analysis. In this way,  $r$  describes the relationship between NDVI and temperature after the effect of precipitation has been removed (Helsel and Hirsch, 2002). Due to the negative relation between temperature and precipitation,  $r$  tends to become more highly significant after eliminating the rainfall influence (Supplementary Fig. S2). Monthly temperature residuals were obtained by simple linear regression of monthly mean temperature with current month rainfall. Shinoda and Nandintsetseg (2011) reported that the period of soil moisture in the Mongolian steppe can be as long as 8.2 months, which implies that signals of the previous year's rainfall should be found in the current year's vegetation. Considering lag effects of rainfall on vegetation and spatial

differences, six monthly rainfall totals (the current month and five previous months) were chosen as potential explanatory variables in a multiple linear regression with monthly mean NDVI.

IMSL\_ALLBEST procedure in the IDL (IDL, Interactive Data Language) software was used with adjusted  $r^2$  as the criterion, to select the best multiple linear regression models for each pixel. Regression diagnostics were then performed by correlation analysis of monthly NDVI residuals versus other candidate explanatory variables, e.g. the previous annual rainfall. High correlation coefficients indicate that there is a significant rainfall signal left in the NDVI residuals. As such, a further linear regression of the NDVI residuals was applied against the explanatory variable to obtain the final monthly NDVI residuals.

With respect to the correlation analysis between NDVI and precipitation, we used the original data to determine the  $r$ .

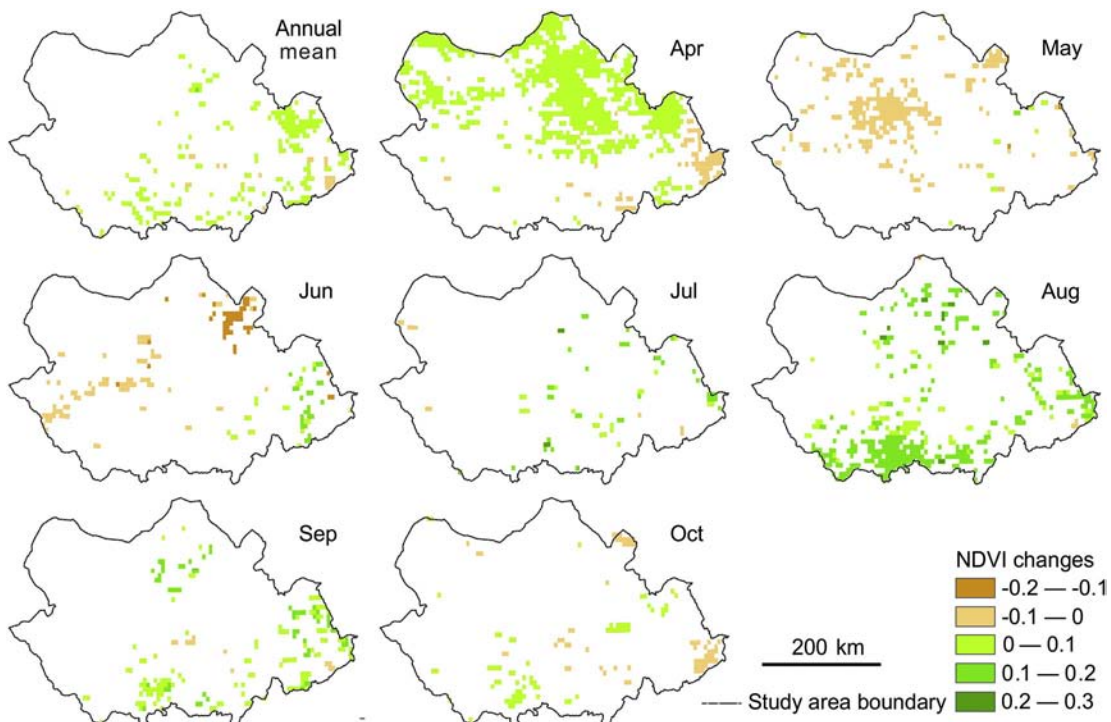


**Fig. 3.** Annual and monthly NDVI changes for the period 1982–2006 ( $p < 0.05$ ).

With respect to the relatively coarse resolution of the NDVI dataset, we selected four widely distributed vegetation types including desert steppe, arid steppe, shrub and forest for the correlation analysis, with woody shrub and forest merged into one group. The dune field, where several vegetation types occur, was also treated as one group in the analysis.

3.2.3. Temporal residual trend analysis

We used residual trend analysis (RESTREND) proposed by Evans and Geerken (2004) to determine the causes for the vegetation variations (see also; Herrmann et al., 2005; Huber et al., 2011; Wessels et al., 2007). This method calculates a linear regression for each pixel with precipitation as the independent variable and the NDVI as the explanatory variable, with residuals calculated and regressed against time. Increasing and decreasing residual trends indicate positive and negative impacts on the NDVI brought by other factors, respectively.

4. Results

4.1. Changes of regional climate

Analysis of meteorological records shows a statistically significant warming trend in the study area with the increase of mean annual temperature of 1–2.5 °C during the period 1982 to 2006. The rising trend varied from month-to-month with significant increases occurring primarily in February, March, July and September. February experienced the highest warming rate with a mean temperature increase between 3 and 5.5 °C (Table 1). The warming magnitude decreased southward and is more punctuated in the drier west (Supplementary Fig. S3). In contrast with temperature changes, both the annual and monthly precipitation in the study area fluctuated over time without any statistically significant trend. Nevertheless, climate underwent a slightly wetter phase in the 1990s owing to the relatively abundant precipitation in July and August (Supplementary Fig. S3).

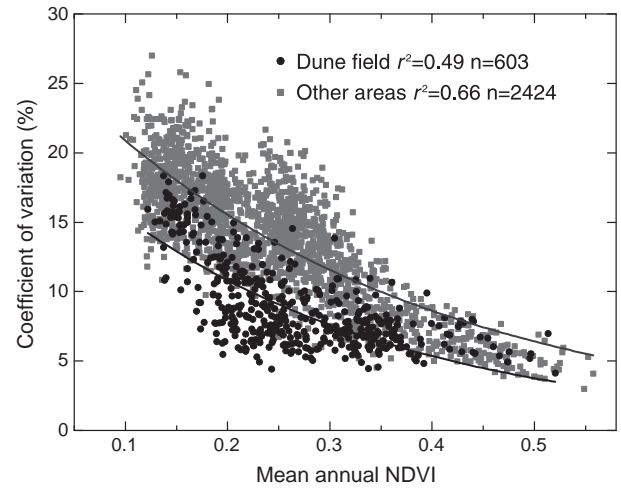


Fig. 5. Coefficient of variation of the annual growing season NDVI.

4.2. NDVI variations

NDVI exhibited a similar variation pattern with precipitation on an annual scale. A substantial greening trend occurred in the 1990s corresponding with wetter climate (Fig. 2). Although the increasing trend ceased beginning in 2000, vegetation exhibits a greening trend on an annual scale with significantly increased and decreased NDVI areas accounting for 7% and 0.6% of the entire study area, respectively (Fig. 3). The greening trend is primarily found in scattered areas in the wetter middle and east portions of the study area.

Monthly NDVI displays temporal-specific trends. Significantly increased greenness occurred widely in April and August (25.6% and 13.6% of the study area, respectively; Fig. 3). Both NDVI anomalies and greening deviation curves in April display a remarkable rise since 2001, whereas the NDVI of greening area in August has increased

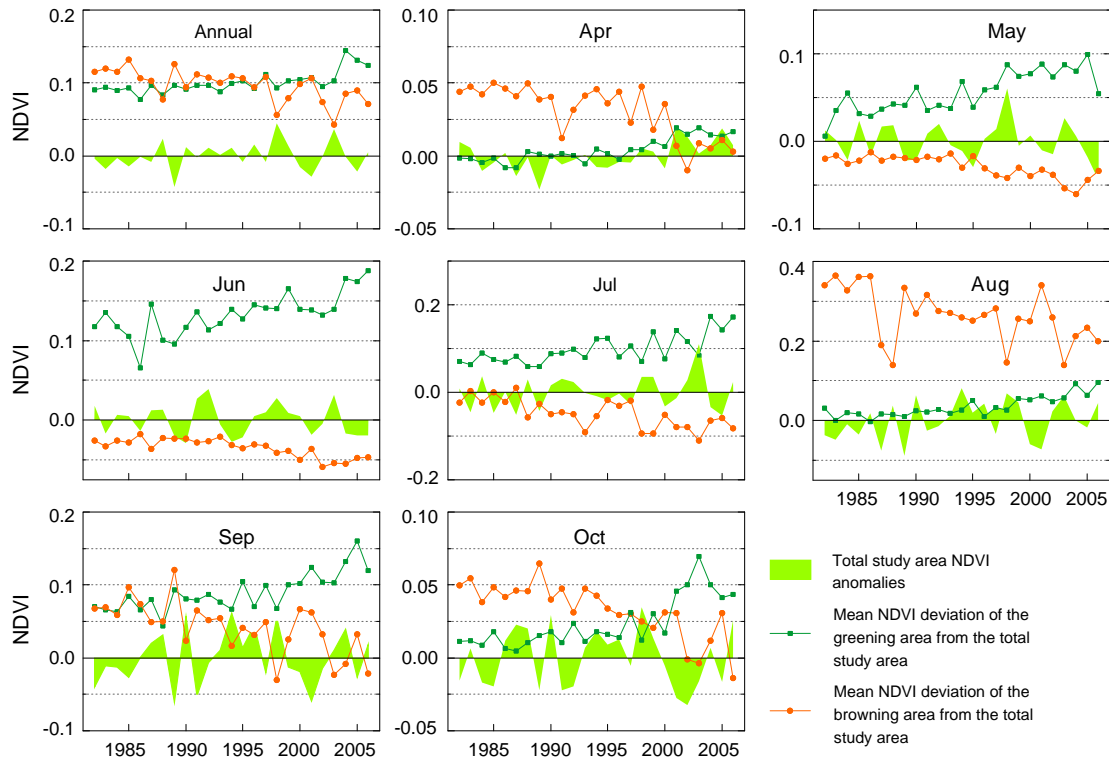
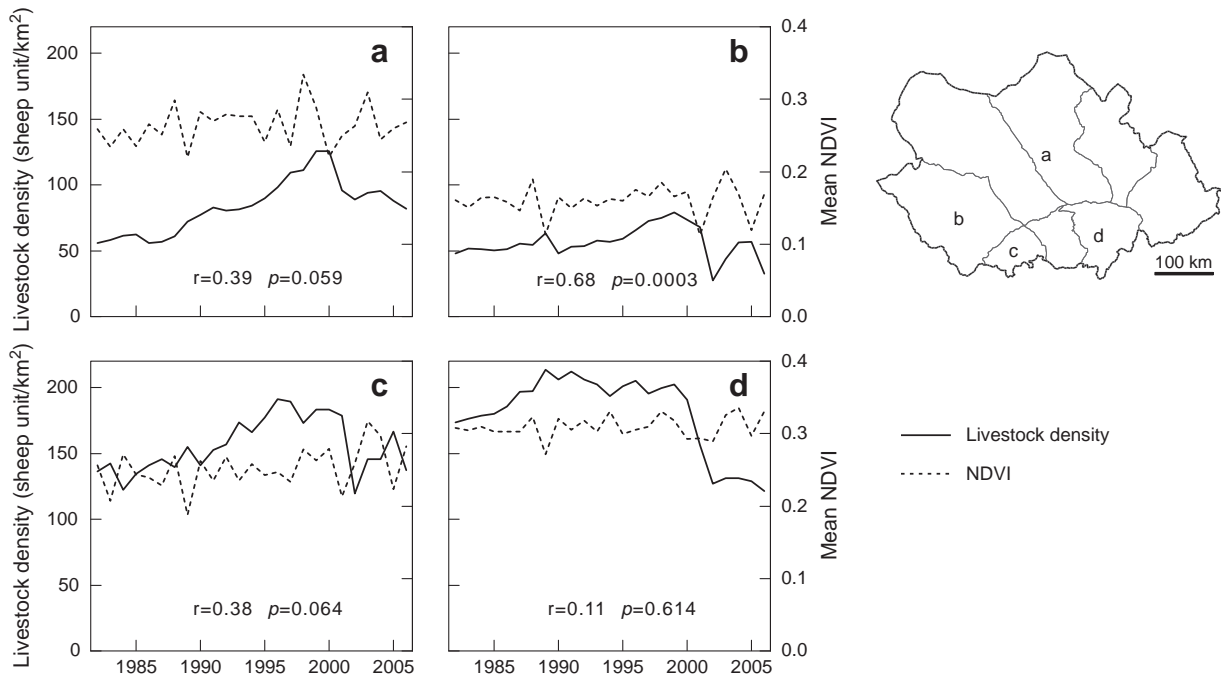


Fig. 4. Time series of the monthly NDVI for the period 1982–2006. The deviation is obtained by subtracting the average NDVI of the significantly greening/browning area ( $p < 0.05$ , see Fig. 3) from the average NDVI of the study area. (For interpretation of the references to color in this figure legend, the reader is referred to the web version of this article.)



**Fig. 6.** Time series of livestock density and mean NDVI of four different counties: (a) Abag, (b) Sonid Youqi, (c) Xianghuangqi, and (d) Zhenglanqi. Correlation coefficients ( $r$ ) between livestock density and the mean NDVI of last year as well as  $p$ -value ( $p$ ) are also given in the figure.

relative to the study area average since 1990s (Fig. 4). On the other hand, vegetation in May and June experienced significant browning processes in the north and west portions of the study area (Fig. 3). The browning time series suggest that the processes driving NDVI

decrease began in the mid of the 1990s (Fig. 4). Spatially, greening took place primarily in the wetter mid and east, while decreasing NDVI mainly occurred in the drier west and east margin where forest and farmland are located.

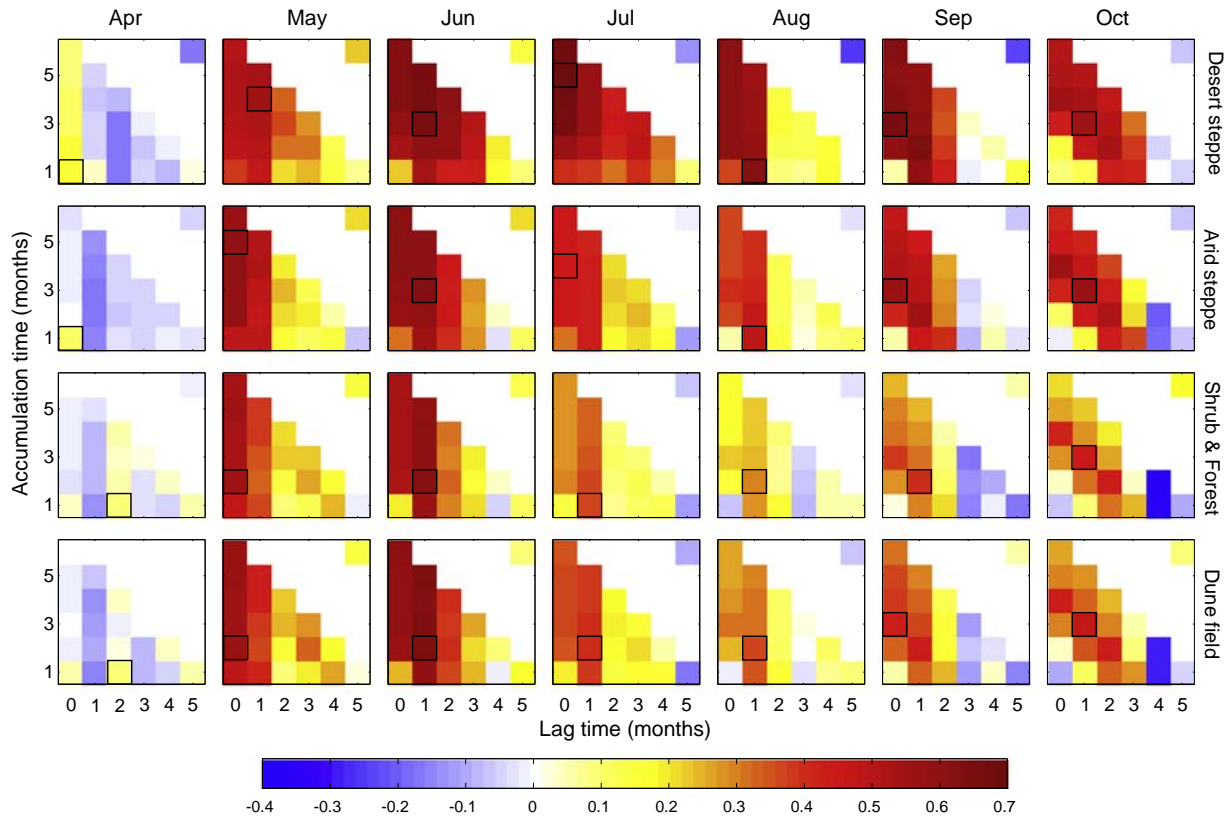


**Fig. 7.** Average correlation coefficients between NDVI and precipitation accumulated over various lengths of time and with different lag times, the framed pixels are the highest values for each group and each month. The upper right pixels for each panels indicate the correlation coefficients between NDVI and the precipitation of the previous year.

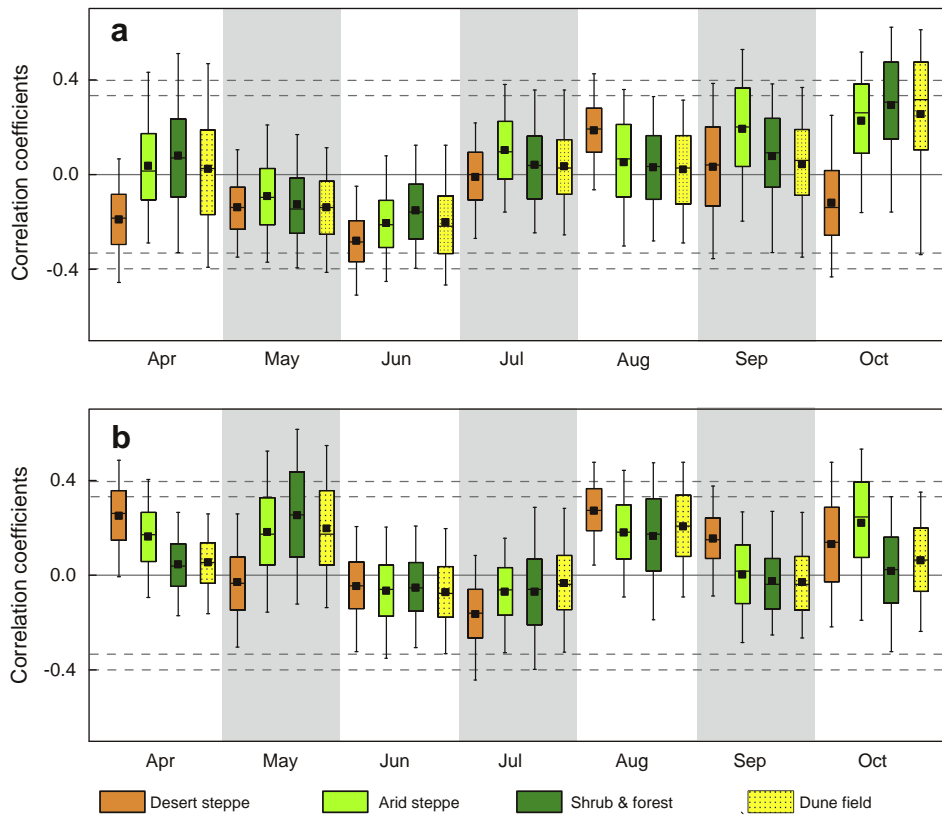


**Fig. 8.** (a) The correlation coefficient between residuals of monthly NDVI and residuals of concurrent month temperature. (b) The same with (a) but the previous month's temperature. The box indicates median, lower and upper quartiles; the solid square in the box represents the mean value; the 5th and 95th percentiles are marked by the bars out of the box. The significance levels of 0.1 and 0.05 are signed by the dashed line.

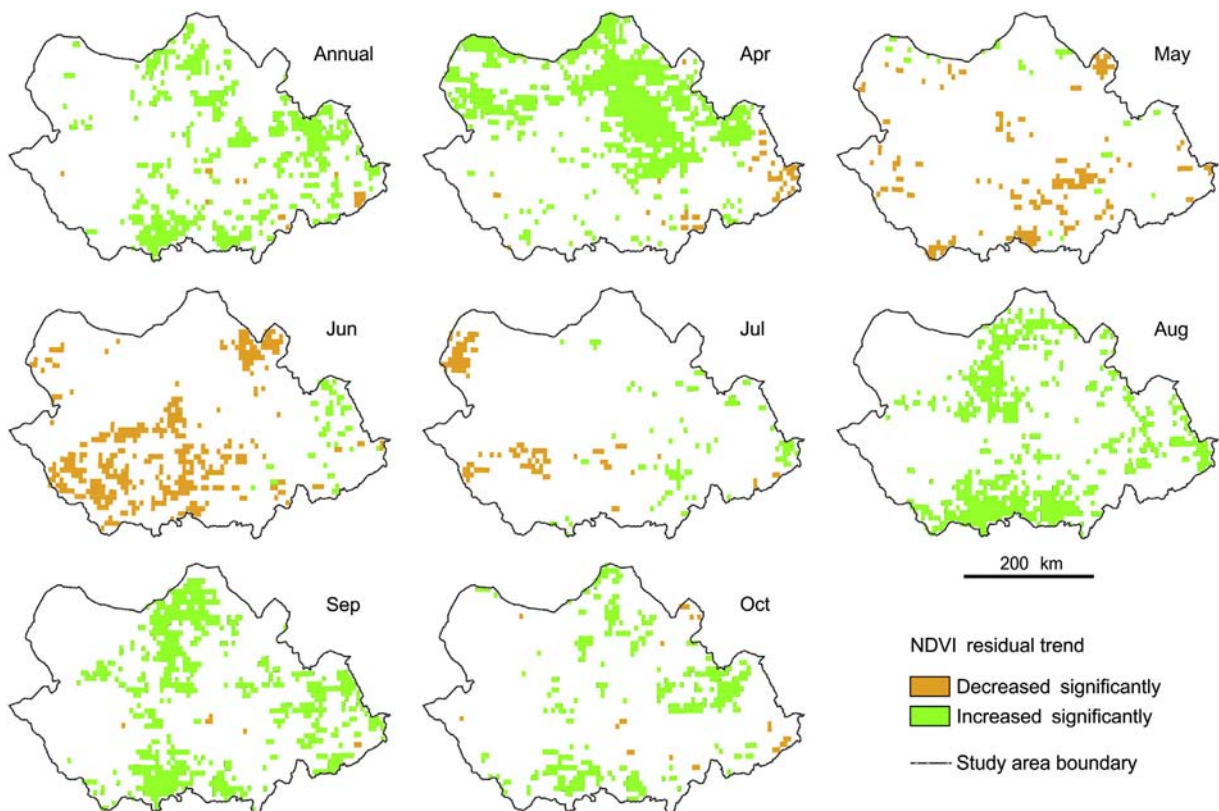


**Fig. 9.** The trends of NDVI residuals obtained from linear regression with precipitation for the period of 1982–2006 ( $p < 0.05$ ).

The variability of the annual NDVI was measured by coefficient of variation (CV) with the CV value ranging from 5% to 27% and correlating negatively with mean annual NDVI. The CV of samples from both dune field and other areas shows a significant exponential decrease with increasing mean annual NDVI (Fig. 5). However, the NDVI of the dune field is much less variable than that of other areas, with a mean CV value of 9% and 14%, respectively.

#### 4.3. Changes of grazing intensity

The grazing intensity in our study area experienced a marked increase in 1990s and then a decline after 2000. In the county of Abag, the livestock density in the late 1990s was twice that of the early 1980s (Fig. 6). Significant changes in grazing intensity are in great contrast with the trendless fluctuations of annual NDVI. Also, the livestock population appears not to vary synchronically with the NDVI on the yearly scale. Rather, it seems that there was a time lag of one year due to the significant correlation between livestock density and the NDVI of the previous year (Fig. 6), suggesting a hysteresis effect of livestock increase in response to the vegetation variations.

#### 4.4. Correlations between NDVI and climate parameters

Correlations between vegetation and precipitation show a spatio-temporal dependence with the highest correlation coefficient occurring in the desert steppe followed by the arid steppe. Shrub and forest vegetation found in the mid east portion of the region shows a more resistant response to precipitation fluctuations. We also note that the NDVI response of dune field areas also displays a low correlation with rainfall, especially in the summer and autumn (Fig. 7). This precipitation restraint on NDVI is most pronounced in May and June as shown by higher  $r$  values and NDVI values during these two months correlate positively with precipitation from the previous year (Fig. 7). A high correlation coefficient between NDVI and precipitation in the desert steppe, however, continues until autumn, whereas it abates for other vegetation types in the relatively rainy months of July and August (Fig. 7).

Pixel based correlation analysis also reveals a lagged effect with monthly NDVI correlated positively with precipitation 4–5 months prior. The highest correlation coefficient found is between NDVI and sum of rainfall for the dune field over a 2–3 month period, whereas monthly NDVI of the desert steppe and arid steppe required a 4–5 month sum of rainfall to obtain the strongest linear association, implying a longer moisture memory in drier areas.

We also found that in general warmer temperatures favored vegetation growth especially in the drier desert steppe. Negative correlations between NDVI and mean temperature in May and June (Fig. 8a), and increasing temperature of these two months also tended to restrain vegetation growth in the following month (Fig. 8b). For the desert steppe areas, besides May and June, NDVI values in April and October also correlate negatively with temperature of that month but positively with temperature of the previous month. As well, for these areas NDVI values of August during rainy years exhibit positive correlation with the temperature of both July and August. For other areas, monthly temperature, except that of May and June, did not display a significantly negative correlation with the NDVI.

#### 4.5. Residual trends (RESTREND)

RESTREND analysis results display a similar pattern but with much greater ranges than that of NDVI (Fig. 9). Significant increases occurred widely in April, August, September and October (as well as in the annual residuals in the mid and east), while a negative trend of residuals primarily appears in drier months of May and June. Although the residual trend of both May and June shows a pronounced decrease, the distribution patterns of these two months are quite different. In May, a negative trend disperses across the entire study area while it is primarily

concentrated in the drier and warmer southwest portion of the study area in June. Decreasing residual trends are also found in the western portion of the study area in July (Fig. 9) when no significant decreasing trend of NDVI was detected (Fig. 3). The distribution patterns of residual trends appear to be related to water availability with negative (positive) trends primarily found in drier (wetter) seasons and subareas.

## 5. Discussion

### 5.1. Potential causes of NDVI variations

#### 5.1.1. Rainfall

A high correlation between NDVI and rainfall is found in dryland vegetation systems globally (Helldén and Tottrup, 2008). In African Sahel, rainfall has been suggested as the dominant cause for a recent widespread increase in the vegetation greenness (Herrmann et al., 2005). We show that NDVI in our study area is well coupled to precipitation especially in the drier west and during May and June (Fig. 7), mirroring the crucial role of water for the vegetation. In the recent decades wetter Julys in 1990s contributed to the increased greenness in August and even September. Precipitation alone, however, could not explain all of the monthly NDVI trends over the period of study, e.g. April, May and June, as no significant trend of precipitation was detected. The similarity of the NDVI trends (Fig. 3) and RESTREND results (Fig. 9) also suggests that precipitation quantity is probably not the single driver of the significant trends of vegetation greenness changes observed.

Relationships between precipitation and NDVI were found to be different for the different vegetation types present in the study area. The lowest correlation coefficient was observed in forest and shrub areas, reflecting their slow reaction to high fluctuations in precipitation. In contrast, the desert steppe exhibited the most pronounced dependence on the rainfall over most of the growing season. This response appears to be related to rooting depth with roots of trees and shrubs reaching the deep soil water that cannot be used by short-rooting grasses (Potter et al., 1998). Besides, the area dominated by woody species received more precipitation. These combined factors may explain the higher dependence on precipitation of steppe than that of forest and shrub.

The dune field area, as reflected by both lower CV (Fig. 5) and  $r$  values with precipitation (Fig. 7) was found to be more stable than the average of the study area. Nevertheless, the lower dependence of dune field vegetation on precipitation mainly occurs in summer (July and August), while in May and June, NDVI displays a significant correlation with precipitation as found in other areas. The seasonal resistance to precipitation variability might not be ascribed to the woody species growing on the dune field, since herb-rich arid steppe and desert steppe vegetation is also found in the dune field (Fig. 1). Instead, this resistance can most likely be attributed to soil type and landform characteristics. Because of coarser soil texture, less water evaporates from the sandy soil than from loams in arid and semi-arid climates (Alizai and Hulbert, 1970; Noy-Meir, 1973). Bare sand surfaces characterized by lower temperatures due to higher albedo (Kidron and Tal, 2012; Qin et al., 2002) also tend to reduce evaporation. Moreover, like other sand seas of China (Yang et al., 2012), channels occurring in the southern margin due to the foreland location of the dune field, imply that water in the dune field might be partially recharged by the ephemeral streams. These factors should enable the dune field to have high water availability suitable for sustaining a more stable vegetation cover than in other areas.

#### 5.1.2. Temperature

Temperature in the study area rose remarkably between 1982 and 2006. It has been reported that the warming climate of northern mid-to-high latitudes benefits vegetation in the spring (Wang et al., 2011). Our results, however, suggest that vegetation greenness in our study area increased significantly only in April whereas it decreased in the

following two months. Further, the greening April in our study area should not be ascribed to the warming late winter/early spring as April NDVI did not increase significantly until 2001 (Fig. 4) and temperature increased gradually. Limited water availability likely explains the limited minor greening associated with warming spring temperatures. During the rainy months of July and August, rising temperatures have not hitherto constrained vegetation growth as inferred from the correlation between temperature and NDVI (Fig. 8).

### 5.1.3. Human activity

In exploring the reasons for vegetation variations, human management, often incriminated as the primary driver for desertification in China, cannot be neglected. Due to the rising price of animal products in 1990s, livestock numbers increased significantly especially in the late 1990s (Fig. 6). Increased grazing pressure results in a less tolerant vegetation response to disturbance. In addition, the asynchrony of livestock population and vegetation production (Fig. 6) exacerbates the pressure on environment when drought occurs and further increases vegetation degradation (Smith et al., 2007).

Pasture land in the study area, originally community-owned, was divided into small patches for each household around mid-1990s. This was followed by building the fences separating family pastures in order to prevent trespassing. Environment conservation programs carried out since 2001 have attempted to rehabilitate vegetation in order to reduce dust storms in Beijing and Tianjin. This program involves a grazing break in the spring, a grazing ban in fragile areas, and reconverting farmland to grassland (our field observations). As a consequence of these practices livestock numbers decreased substantially after 2001 (Fig. 6).

To a certain degree, human management is the trigger for the most significant greening and browning trends in the study area. On the one hand, conservation practices produced positive impacts on vegetation. The most marked evidence is the widely observed significant April vegetation greening since 2001 when the grazing break policy has been implemented (Figs. 3 and 4). The suspension of grazing, however, has had little influence on the vegetation of May and June as the measurement is mainly executed in April. NDVI greening area deviation curves of other months (June, August, September and October) also show a higher value during the last few years (Fig. 4), indicating increases of greenness after the program was initiated. The positive impacts of conservation practices can also be identified from the differential response of the vegetation to droughts before (1989) and after (2005) the implementation of the program. In 1989, annual precipitation and annual NDVI were 31% and 0.04 lower than normal, respectively, while in 2005 NDVI was only 0.02 less than the average even though the precipitation was 41% below the mean annual precipitation (Fig. 2).

At the same time, some human management issues appear to be responsible for decreased NDVI in some months. The coincidence of domestic animal increases (Fig. 6) and browning in May and June (Fig. 4) implies that vegetation changes in these two months might be human induced. In addition, the decrease in NDVI is also coincident with the timing of the increased enclosure of pastoral land. Sneath (1998) suggested that limiting mobility of livestock is associated with the degradation of pasture. In our study area, the herders usually divided their pasture into two parts; one for fodder cultivation and the other for grazing. This practice further restricted livestock movement. Consequently, greater pressure was imposed on grazing lands creating sandy and bare earth in areas that could be potentially covered by vegetation (Fig. 10). Therefore, we believe that human management practices primarily account for diminished NDVI values in May and June, although the extent to which this has resulted from higher livestock numbers or the enclosure of pasture is not clear. Some additional browning trends in the east margin are probably related to farmland abandonment and forest logging.

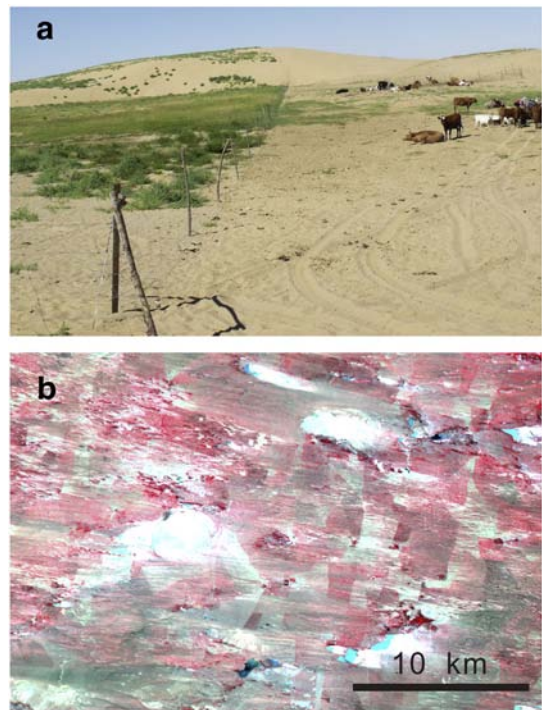


**Fig. 10.** Different land covers separated by the fence in the study area as seen (a) during field investigation and (b) from the Landsat TM image (August 14, 2007). Areas with the most vegetation are in red, the white part is bare sand and the lakes are in blue). (For interpretation of the references to color in this figure legend, the reader is referred to the web version of this article.)

## 5.2. Outlook for the area under the scenario of global warming

Seasonal correlations between vegetation and temperature have been investigated in some earlier studies. Piao et al. (2006b) suggested that temperate steppe vegetation in north China correlated positively with temperature during the entire growing season and the correlation was more significant in spring and autumn than in summer. Wang et al. (2003) pointed out that the vegetation in Kansas (USA) favored warming at both early and end of the growing season, with correlations between NDVI and temperature negative in the middle growing season. Both studies imply that warming could be advantageous to vegetation in summer. However, our study suggests that vegetation in May and June, characterized by negative correlations with temperature and higher correlation coefficients with precipitation as well as significant decrease in NDVI, is more sensitive to rising temperatures. In the rainy summer and following autumn, the relationship between temperature and vegetation growth appears to be positive. In terms of vegetation types, desert steppe appeared to be most strongly impacted by warming climate. The period of negative correlation between temperature and NDVI is longer in desert steppe area (April, May, June and October) than in other zones (roughly May and June). Also, the decreased NDVI mainly occurred in the desert steppe especially in the drier May and June. Although environment conservation projects have been in existence for over six years, little long-lasting effect is currently visible in the desert steppe as evidenced by the small increasing trend of residuals (Fig. 9).

The seasonal vulnerability of vegetation (May and June), possibly obscured by strong vegetation growth in summer (July and August), should not be neglected while assessing vegetation variability and response. NDVI in May and June not only correlates significantly with precipitation of previous months, but also has a positive relationship with the precipitation of the previous year (Fig. 7). Long-term cold season temperatures contribute to the moisture memory and therefore warming in winter and spring could aggravate seasonal moisture shortage. The seasonal browning did restrain vegetation growth in other

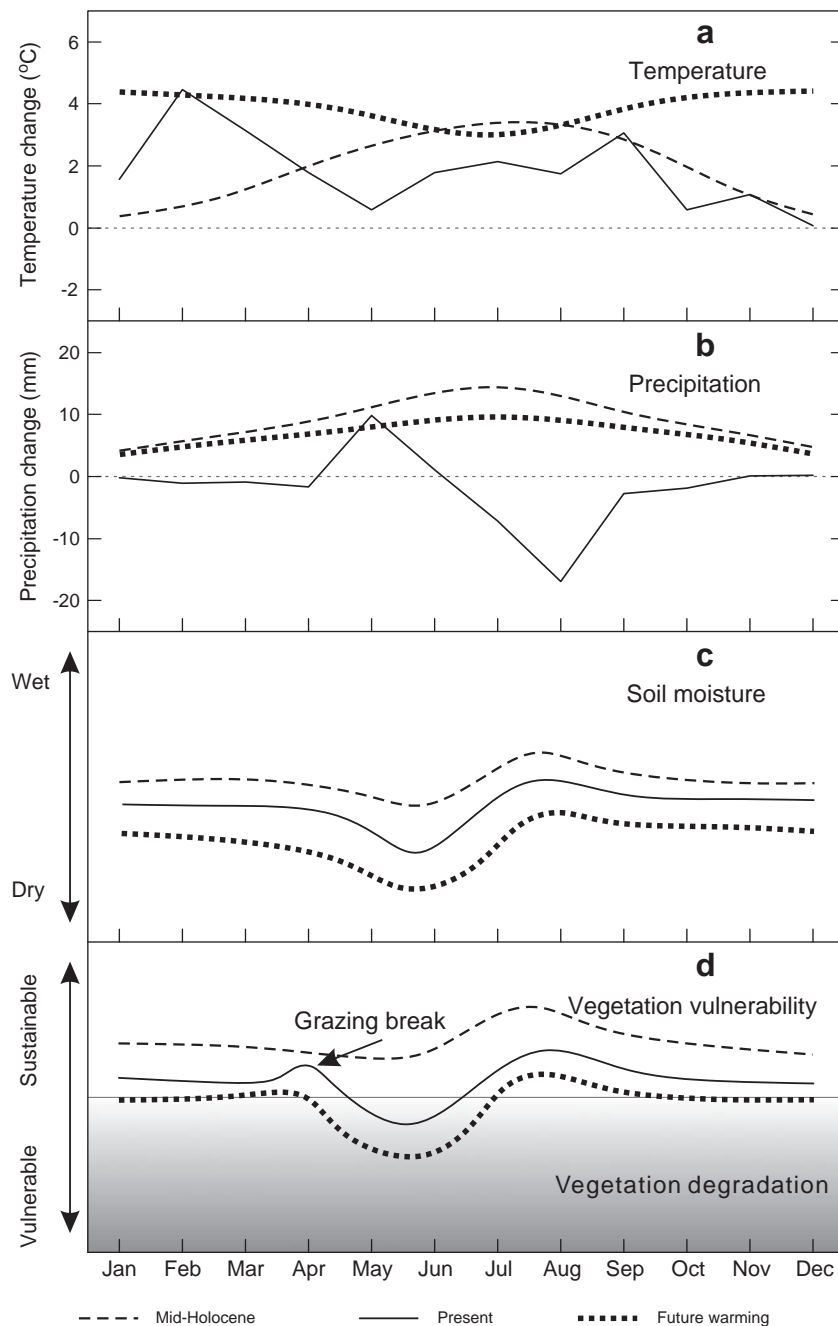


**Fig. 11.** Schematic representation of climate conditions coupled with soil moisture and vegetation status of mid-Holocene, present and future (2080–2099) warming in the study area. The future precipitation and temperature changes are based on A1B scenario for the period 2080–2099 (IPCC, 2007). The mid-Holocene temperature curve is a synthesis of Dallmeyer et al. (2010), Jiang et al. (2012) and Renssen et al. (2012), whereas the precipitation of mid-Holocene is from Yang et al. (2013). The present temperature and precipitation changes (1982–2006) are from this study. It should be noted that the present precipitation trends for each month are not statistically significant.

months so that only 10% and 7.9% of the area having experienced decreased NDVI in May and June display an increased greenness in the widespread greening months of April and August, respectively. In the drier west, RESTREND shows that additional factors, such as temperature and human activities, have induced the significant decrease of NDVI even during the rainy month of July (Fig. 9). This might be an early indicator of an emergent extension of dry intervals in response to global warming.

In addition to the modern monitoring, paleoclimatic records can provide an analog for assessing the impacts of global warming on vegetation in the study area. Driven by the higher insolation in the summer, the early and mid-Holocene (10,000–3000 years BP) were characterized by higher global temperatures (Marcott et al., 2013). Associated

with warmer climate, a paleosol not only developed in the eastern portion of the study area (Mason et al., 2009; Yang et al., 2008) but also occurs in the west part where sparse vegetation grows today (Yang et al., 2013). The paleosol characterized by high organic carbon content, indicates a much denser vegetation cover during early and mid-Holocene over the area. However, the well-vegetated environments should not be attributed to the higher temperature only. Yang et al. (2013) estimated that the annual precipitation of the Hunshandake Sandy Land during 9.6–3 ka could be 30–140 mm more than at present. Considering the development of the dark paleosol, the temperature may not have been much higher. Wen et al. (2010) suggested the annual temperature during the Holocene in the Hulun Lake basin, approximately 500 km NNE of the study area, could have not been over 1 °C higher than nowadays.

Simulations indicate that the monthly maximum positive temperature anomaly relative to preindustrial level in the study area during the Holocene was ca. 3 °C (Renssen et al., 2012). Increased precipitation which offsets the enhancement of evapotranspiration resulting from a moderately warming climate would have been critical for the formation of this paleosol.

The temperature and rainy season precipitation in this area are projected to increase by 2.5–5 °C and 10–20% respectively (20–80 mm) by the end of the century (IPCC, 2007). Thus, it is unlikely that vegetation cover levels similar to that found during the middle Holocene will occur under the global warming. Furthermore, we note that the warm climate in the Holocene is different from the anthropogenic warming in the future primarily due to seasonality changes. Due to orbital forcing, the largest positive deviation of temperature occurred in summer during the early to mid-Holocene, whereas the temperature of the dry season, namely winter and spring, would be lower than at present during the mid-Holocene (Dallmeyer et al., 2010; Jiang et al., 2012; Renssen et al., 2012). The seasonality, in addition to the rainy climate, should have contributed to a well-vegetated early and mid-Holocene. Thus, global warming in this century, which is characterized with the rising temperature all the year round, cannot benefit vegetation rehabilitation and reestablishment in this area (Fig. 11).

## 6. Conclusions

Our statistical analysis of weather records from 17 stations in the Xilin Gol district of Inner Mongolia demonstrates that the increase in mean annual temperature from 1982 to 2006 is greater in the arid northwest than in the subhumid southeast, ranging from 1 °C to 2.6 °C. There is a clear monthly difference in terms of temperature increase rate and the highest monthly increase occurs in February, reaching as much as 3–5.5 °C. Under the warming climate, our findings show that there is little area that has experienced significant decreases in NDVI in the entire district during the study period probably due to the slight increase in rainfall in the 1990s and more recent desertification control efforts. This result is different from several earlier studies that reported that Xilin Gol has undergone severe desertification during past decades. This discrepancy could be attributed to the difference in the selection of data and approaches.

Warming climate, in contrast to other studies, has not promoted vegetation growth in the spring; instead, the greenness displayed a decrease in May and June. Although this seasonal browning is associated with human management, limited water availability in late spring and early summer is likely the root cause and ongoing warming would likely exacerbate this seasonal moisture shortage. For the desert steppe, we identified a negative response of NDVI to increased temperature in both spring and autumn, and the conservation program seems to have produced few positive effects in these areas. This result suggests that desert steppe will possibly be the most fragile vegetation type in a warmer world. The warming in this century differs from the warmer climate during the early and middle Holocene with respect to magnitude and seasonality, both of which would be not favorable to the vegetation in the entire region in the future. Even if a much more intense rehabilitation effort is envisioned, it is unlikely that a reoccurrence of mid-Holocene vegetation cover levels will occur in the temperate drylands of East Asia under current warming trends.

## Acknowledgments

This research was supported by the National Natural Science Foundation of China (grant nos.: 40930105, 41172325) and the CAS Strategic Priority Research Program (grant no.: XDA05120502). We also thank Meteorological Administration of China and local Meteorological Administrations for providing the climate data. Sincere thanks are extended to the local residents and governments for providing socio-economic information, to Prof. Louis Scuderi, anonymous reviewers and Editor

Prof. Erik Cammeraat for constructive comments. We thank Prof. Louis Scuderi also for having duly corrected the English language.

## Appendix A. Supplementary data

Supplementary data to this article can be found online at <http://dx.doi.org/10.1016/j.catena.2014.03.003>.

## References

- Alizai, H.A., Hulbert, L.C., 1970. Effects of soil texture on evaporative loss and available water in semi-arid climates. *Soil Sci.* 110, 328–332.
- Beck, H.E., McVicar, T.R., van Dijk, A.I.J.M., Schellekens, J., de Jeu, R.A.M., Bruijnzeel, L.A., 2011. Global evaluation of four AVHRR-NDVI data sets: intercomparison and assessment against Landsat imagery. *Remote Sens. Environ.* 115, 2547–2563.
- Box, E.O., Holben, B.N., Kalb, V., 1989. Accuracy of the AVHRR vegetation index as a predictor of biomass, primary productivity and net CO<sub>2</sub> flux. *Vegetatio* 80, 71–89.
- Brown, R.D., 2000. Northern hemisphere snow cover variability and change, 1915–97. *J. Clim.* 13, 2339–2355.
- CCICCD, 2000. China National Report on the Implementation of United Nations Convention to Combat Desertification and National Action Programme to Combat Desertification. China National Committee for the Implementation of the UNCCD, Beijing.
- CCICCD, 2006. China National Report on the Implementation of the United Nations Convention to Combat Desertification. China National Committee for the Implementation of the UNCCD, Beijing.
- China Meteorological Data Sharing Service System, m. Surface meteorological dataset of international exchange stations of China (daily). Available online: <http://new-cdc.cma.gov.cn:8081/home.do> (in Chinese, access on 23 March 2011).
- Dai, A., 2011. Drought under global warming: a review. *Wiley Interdiscip. Rev. Clim. Chang.* 2, 45–65.
- Dallmeyer, A., Claussen, M., Otto, J., 2010. Contribution of oceanic and vegetation feedbacks to Holocene climate change in monsoonal Asia. *Clim. Past* 6, 195–218.
- Editorial Board of Vegetation Map of China, Chinese Academy of Sciences, 2007. Vegetation Map of The People's Republic of China (1:1,000,000). Geological Press, Beijing (in Chinese).
- Evans, J., Geerken, R., 2004. Discrimination between climate and human-induced dryland degradation. *J. Arid Environ.* 57, 535–554.
- Galton, F., 1886. Regression towards mediocrity in hereditary stature. *J. Anthropol. Inst. G. B. Irel.* 15, 246–263.
- Global Land Cover Facility (GLCF), . The GIMMS (Global Inventory Modeling and Mapping Studies) data set. Available online <ftp://ftp.glcfc.umd.edu/glcfc/GIMMS/Geographic> (access on 20 January 2011).
- Heldén, U., Tottrup, C., 2008. Regional desertification: a global synthesis. *Global Planet. Chang.* 64, 169–176.
- Helsel, D.R., Hirsch, R.M., 2002. Statistical methods in water resources, 323. US Geol. Surv. (<<http://water.usgs.gov/pubs/twri/twri4a3/>>).
- Herrmann, S.M., Anyamba, A., Tucker, C.J., 2005. Recent trends in vegetation dynamics in the African Sahel and their relationship to climate. *Glob. Environ. Chang.* 15, 394–404.
- Huber, S., Fensholt, R., Rasmussen, K., 2011. Water availability as the driver of vegetation dynamics in the African Sahel from 1982 to 2007. *Global Planet. Chang.* 76, 186–195.
- Hulme, M., 2001. Climatic perspectives on Sahelian desiccation: 1973–1998. *Glob. Environ. Chang.* 11, 19–29.
- IPCC, 2007. Climate Change 2007 – The Physical Science Basis: Working Group I Contribution to the Fourth Assessment Report of the IPCC, 4. Cambridge University Press, Cambridge, UK.
- Jiang, D., Lang, X., Tian, Z., Wang, T., 2012. Considerable model–data mismatch in temperature over China during the mid-Holocene: results of PMIP simulations. *J. Clim.* 25, 4135–4153.
- Kendall, M., 1975. Rank Correlation Methods. Charles Griffin, London.
- Kidron, G.J., Tal, S.Y., 2012. The effect of biocrusts on evaporation from sand dunes in the Negev Desert. *Geoderma* 179, 104–112.
- Lei, Y., Duan, A., 2011. Prolonged dry episodes and drought over China. *Int. J. Climatol.* 31, 1831–1840.
- Liu, Z., Yang, X., 2013. Geochemical–geomorphological evidence for the provenance of aeolian sands and sedimentary environments in the Hunshandake Sandy Land, eastern Inner Mongolia, China. *Acta Geol. Sin.* 87, 871–884 (English Edition).
- Liu, H., Zhou, C., Cheng, W., Long, E., Li, R., 2008. Monitoring sandy desertification of the Otindag Sandy Land based on multi-date remote sensing images. *Acta Ecol. Sin.* 28, 627–635.
- Ma, Z., Fu, C., 2006. Some evidence of drying trend over northern China from 1951 to 2004. *Chin. Sci. Bull.* 51, 2913–2925.
- Mann, H.B., 1945. Nonparametric tests against trend. *Econometrica J. Econ. Soc.* 245–259.
- Marcott, S.A., Shakun, J.D., Clark, P.U., Mix, A.C., 2013. A reconstruction of regional and global temperature for the past 11,300 years. *Science* 339, 1198–1201.
- Mason, J.A., Lu, H., Zhou, Y., Miao, X., Swinehart, J.B., Liu, Z., Goble, R.J., Yi, S., 2009. Dune mobility and aridity at the desert margin of northern China at a time of peak monsoon strength. *Geology* 37, 947–950.
- Millennium Ecosystem Assessment, 2005. Ecosystems and Human Well-being: Desertification Synthesis. World Resources Institute, Washington, DC.
- Ministry of Agriculture of People's Republic of China, 2002. Agricultural Standards of People's Republic of China: Calculation of Proper Carrying Capacity of Rangelands. China Standards Press, Beijing.

- Myneni, R.B., Hall, F.G., Sellers, P.J., Marshak, A.L., 1995. The interpretation of spectral vegetation indexes. *IEEE Trans. Geosci. Remote Sens.* 33, 481–486.
- Nemani, R.R., Keeling, C.D., Hashimoto, H., Jolly, W.M., Piper, S.C., Tucker, C.J., Myneni, R.B., Running, S.W., 2003. Climate-driven increases in global terrestrial net primary production from 1982 to 1999. *Science* 300, 1560–1563.
- Nicholson, S.E., 2001. Climatic and environmental change in Africa during the last two centuries. *Clim. Res.* 17, 123–144.
- Noy-Meir, I., 1973. Desert ecosystems: environment and producers. *Annu. Rev. Ecol. Evol. Syst.* 4, 25–51.
- Paruelo, J.M., Epstein, H.E., Lauenroth, W.K., Burke, I.C., 1997. ANPP estimates from NDVI for the central grassland region of the United States. *Ecology* 78, 953–958.
- Pearson, K., 1920. Notes on the history of correlation. *Biometrika* 13, 25–45.
- Peng, S., Piao, S., Ciais, P., Fang, J., Wang, X., 2010. Change in winter snow depth and its impacts on vegetation in China. *Glob. Chang. Biol.* 16, 3004–3013.
- Piao, S., Fang, J., Liu, H., Zhu, B., 2005. NDVI-indicated decline in desertification in China in the past two decades. *Geophys. Res. Lett.* 32, L06402.
- Piao, S., Fang, J., Zhou, L., Ciais, P., Zhu, B., 2006a. Variations in satellite-derived phenology in China's temperate vegetation. *Glob. Chang. Biol.* 12, 672–685.
- Piao, S., Mohammat, A., Fang, J., Cai, Q., Feng, J., 2006b. NDVI-based increase in growth of temperate grasslands and its responses to climate changes in China. *Glob. Environ. Chang.* 16, 340–348.
- Pinzon, J., Brown, M.E., Tucker, C.J., 2005. Satellite time series correction of orbital drift artifacts using empirical mode decomposition. In: Huang, N. (Ed.), *Hilbert–Huang Transform: Introduction and Applications*, pp. 167–186.
- Potter, D.U., Gosz, J.R., Molles Jr., M.C., Scuderi, L.A., 1998. Lightning, precipitation and vegetation at landscape scale. *Landsc. Ecol.* 13, 203–214.
- Qin, Z., Berliner, P., Karnieli, A., 2002. Micrometeorological modeling to understand the thermal anomaly in the sand dunes across the Israel–Egypt border. *J. Arid Environ.* 51, 281–318.
- Renssen, H., Seppa, H., Crosta, X., Goosse, H., Roche, D.M., 2012. Global characterization of the Holocene thermal maximum. *Quat. Sci. Rev.* 48, 7–19.
- Sen, P.K., 1968. Estimates of the regression coefficient based on Kendall's tau. *J. Am. Stat. Assoc.* 63, 1379–1389.
- Shinoda, M., Nandintsetseg, B., 2011. Soil moisture and vegetation memories in a cold, arid climate. *Global Planet. Chang.* 79, 110–117.
- Slayback, D.A., Pinzon, J.E., Los, S.O., Tucker, C.J., 2003. Northern hemisphere photosynthetic trends 1982–99. *Glob. Chang. Biol.* 9, 1–15.
- Smith, D.M.S., McKeon, G.M., Watson, I.W., Henry, B.K., Stone, G.S., Hall, W.B., Howden, S.M., 2007. Learning from episodes of degradation and recovery in variable Australian rangelands. *Proc. Natl. Acad. Sci.* 104, 20690–20695.
- Sneath, D., 1998. State policy and pasture degradation in Inner Asia. *Science* 281, 1147–1148.
- Stein, M.L., 1999. *Interpolation of Spatial Data: Some Theory for Kriging*. Springer Verlag, New York.
- Theil, H., 1992. A rank-invariant method of linear and polynomial regression analysis. In: Raj, B., Koerts, J. (Eds.), *Henri Theil's Contributions to Economics and Econometrics*. Springer, pp. 345–381.
- Tucker, C.J., 1979. Red and photographic infrared linear combinations for monitoring vegetation. *Remote Sens. Environ.* 8, 127–150.
- Tucker, C.J., Slayback, D.A., Pinzon, J.E., Los, S.O., Myneni, R.B., Taylor, M.G., 2001. Higher northern latitude Normalized Difference Vegetation Index and growing season trends from 1982 to 1999. *Int. J. Biometeorol.* 45, 184–190.
- Tucker, C.J., Pinzon, J.E., Brown, M.E., Slayback, D.A., Pak, E.W., Mahoney, R., Vermote, E.F., El Saleous, N., 2005. An extended AVHRR 8-km NDVI dataset compatible with MODIS and SPOT vegetation NDVI data. *Int. J. Remote Sens.* 26, 4485–4498.
- Walter, H., Lieth, H., 1960. *Klimadiagramm-weltatlas*. G. Fischer, Jena.
- Wang, J., Rich, P., Price, K., 2003. Temporal responses of NDVI to precipitation and temperature in the central Great Plains, USA. *Int. J. Remote Sens.* 24, 2345–2364.
- Wang, J., Rich, P.M., Price, K.P., Kettle, W.D., 2004a. Relations between NDVI and tree productivity in the central Great Plains. *Int. J. Remote Sens.* 25, 3127–3138.
- Wang, T., Wu, W., Xue, X., Han, Z., Zhang, W., Su, Q., 2004b. Spatial-temporal changes of sandy desertified land during last 5 decades in northern China. *Acta Geograph. Sin.* 59, 203–212.
- Wang, X., Piao, S., Ciais, P., Li, J., Friedlingstein, P., Koven, C., Chen, A., 2011. Spring temperature change and its implication in the change of vegetation growth in North America from 1982 to 2006. *Proc. Natl. Acad. Sci.* 108, 1240–1245.
- Wen, R., Xiao, J., Chang, Z., Zhai, D., Xu, Q., Li, Y., Itoh, S., 2010. Holocene precipitation and temperature variations in the East Asian monsoonal margin from pollen data from Hulun Lake in northeastern Inner Mongolia, China. *Boreas* 39, 262–272.
- Wessels, K.J., Prince, S.D., Malherbe, J., Small, J., Frost, P.E., VanZyl, D., 2007. Can human-induced land degradation be distinguished from the effects of rainfall variability? A case study in South Africa. *J. Arid Environ.* 68, 271–297.
- Yang, X., Ding, Z., Fan, X., Zhou, Z., Ma, N., 2007. Processes and mechanisms of desertification in northern China during the last 30 years, with a special reference to the Hunshandake Sandy Land, eastern Inner Mongolia. *Catena* 71, 2–12.
- Yang, X., Zhu, B., Wang, X., Li, C., Zhou, Z., Chen, J., Wang, X., Yin, J., Lu, Y., 2008. Late Quaternary environmental changes and organic carbon density in the Hunshandake Sandy Land, eastern Inner Mongolia, China. *Global Planet. Chang.* 61, 70–78.
- Yang, X., Li, H., Conacher, A., 2012. Large-scale controls on the development of sand seas in northern China. *Quat. Int.* 250, 74–83.
- Yang, X., Wang, X., Liu, Z., Li, H., Ren, X., Zhang, D., Ma, Z., Rioual, P., Jin, X., Scuderi, L., 2013. Initiation and variation of the dune fields in semi-arid China – with a special reference to the Hunshandake Sandy Land, Inner Mongolia. *Quat. Sci. Rev.* 78, 369–380.
- Yu, F., Price, K.P., Ellis, J., Shi, P., 2003. Response of seasonal vegetation development to climatic variations in eastern central Asia. *Remote Sens. Environ.* 87, 42–54.
- Yue, S., Pilon, P., Cavadias, G., 2002. Power of the Mann–Kendall and Spearman's rho tests for detecting monotonic trends in hydrological series. *J. Hydrol.* 259, 254–271.
- Zhong, D., 1999. The dynamic changes and trends of modern desert in China. *Adv. Earth Sci.* 14, 229–234 (in Chinese, with English abstract).
- Zhu, Z., Wang, T., 1990. An analysis on the trend of land desertification in northern China during the last decade based on examples from some typical areas. *Acta Geograph. Sin.* 45, 430–440 (in Chinese, with English abstract).
- Zhu, Z., Wu, Z., Liu, S., Di, X., 1980. *An Outline of Chinese Deserts*. Science Press, Beijing (in Chinese).
- Zou, X., Zhai, P., Zhang, Q., 2005. Variations in droughts over China: 1951–2003. *Geophys. Res. Lett.* 32, L04707.